



# A Thermal Management System to Support Biological Payloads: an Experimental Assessment of Escherichia Coli

---

Pedro Llanos, Hugo Castillo, Parker Mann, Rachel Scruggs and  
Alexander Pepin

EasyChair preprints are intended for rapid  
dissemination of research results and are  
integrated with the rest of EasyChair.

September 10, 2024

# A Thermal Management System to Support Biological Payloads: An Experimental Assessment of *Escherichia coli*

Pedro J. Llanos<sup>1</sup> and Hugo Castillo<sup>2</sup>

*Embry-Riddle Aeronautical University, Daytona Beach, Florida, 32114*

Parker Mann<sup>3</sup>, Rachel Scruggs<sup>4</sup>, and Alexander Pepin<sup>5</sup>

*Embry-Riddle Aeronautical University, Daytona Beach, Florida, 32114*

Researchers conducting space research, particularly those sending payloads to the ISS or during parabolic flights must have a tight temperature control for the optimal growth of all biological models and increase their viability, leveraging the efforts of long-duration spaceflights aboard prospective payloads, free flyers beyond low earth orbit, the Lunar Gateway, and beyond. This paper discusses the performance of an active thermal control system design and provides details on preliminary optimization methods performed to maintain a prescribed thermal environment for sensitive biological payloads (eg. *Escherichia coli*). The thermal pad application times and desired temperature settings are varied, system responses are recorded and recommendations for hardware and software systems are identified to mature such technologies which can be scaled down for prospective biological systems with tight temperature-sensitive profiles on prospective suborbital and orbital payload missions. Our results indicate that our system can target temperatures ranging from about 22°C to 40°C with less than 1°C average error and maintain such thermal profiles when exposed to different environmental conditions. The estimation of bacterial cell count from optical density at 630 nm in wavelength and from the total number of viable cells (colony-forming units) will be provided using our thermal management system and a microbiological incubator set at a fixed temperature. The length of the experiments can last between 12 hours and 48 hours, but the thermal system can run for longer periods. Preliminary *Escherichia coli* optical density results for 12-hour tests at 30°C show an 8%-10% average error across all samples. About 80% of the samples suggest that *Escherichia coli* grew faster in the thermal system than in the incubators. The goal is to obtain a more stable thermal profile while reducing the optical density error to less than 5% across all samples among the thermal system and incubators.

## Nomenclature

ABS	= acrylonitrile butadiene styrene
CFU	= colony forming units
CuSP	= Cubesat to Study Solar Particles
E. Coli	= <i>Escherichia coli</i>
ISS	= International Space Station
LCD	= liquid crystal display
NanoLab	= 20cm × 20cm × 10cm (length × width × height)
NASA	= National Aeronautics and Space Administration
OC	= overnight cultures
OD	= optical density
PATO Lab	= Payload Applied Technology and Operations Lab

---

<sup>1</sup> Associate Professor Space Operations, Applied Aviation Sciences, College of Aviation, 1 Aerospace Blvd.

<sup>2</sup> Assistant Professor, Human Factors and Neurobiology, College of Arts and Sciences, 1 Aerospace Blvd.

<sup>3</sup> Aerospace Physiology undergraduate student, Human Factors and Neurobiology, College of Arts and Sciences.

<sup>4</sup> Spaceflight Operations undergraduate student, Applied Aviation Sciences Department, College of Aviation.

<sup>5</sup> Spaceflight Operations undergraduate student, Applied Aviation Sciences Department, College of Aviation.

SM Lab = Space Microbiology Lab  
TBT = thermal biological test

## I. Introduction

THIS paper addresses an important concern for biology researchers doing space research, particularly those sending payloads to the ISS or during parabolic flights. Temperature control is essential for the optimal growth of all biological models and even though most organisms grow within a temperature range, its fluctuation can influence, greatly, physiological and genetic responses that can interfere with the endpoint(s) measured as part of the experimental plan. This engineering design device or thermal management system would provide tight control over temperature during different stages of the experiment and even under circumstances relevant to space research such as components handling during flight preparation.

For example, in recent Artemis mission, NASA's Orion spacecraft carried some biological experiments on plant seeds to characterize how spaceflight affects nutrient stores, photosynthetic algae to identify genes that contribute to its survival in deep space, the fungus *Aspergillus* to investigate radioprotective effects of melanin and DNA damage response, and yeast used as a model organism to identify genes that enable adaptations to conditions in both low Earth orbit and deep space. Due to the extensive delays with the Artemis launch, the CubeSats housing some of these experiments had been sitting for weeks and could not be recharged. Thus, their batteries may have run down or been affected by temperature fluctuations. The NASA-funded CubeSat to Study Solar Particles (CuSP) showed a spike in battery temperature shortly after its deployment, and researchers have not heard from it since, which prevented it from performing the maneuvers needed to reach a specific orbit. Although the batteries of some CubeSats could be recharged, it was decided that doing so was too high a risk; their power budget depended on their solar panels, assuming they were in a functional state. Because of this, the CubeSats' earthbound science may not produce as much science as planned. With the multiple delays, some of the biological components of these payloads were exposed to environmental elements, such as temperature fluctuations, that could have compromised their viability, therefore adding stress not considered by the researchers. Any microbiology or biology lab will go to lengths to ensure that organisms grow under optimal conditions, and this thermal design instrument would contribute to that.

A further catalyst driving the development of this thermal management system is the need to streamline the transport logistics for a wide array of biological payloads. These payloads often journey from university facilities to various launch sites, such as the West Texas Launch Site for suborbital flights and the Kennedy Space Center for orbital flights. The system aims to minimize temperature fluctuations and negate the need for manual temperature regulation during transit. This enhancement in transportation conditions is pivotal for ensuring these biological systems' survival and optimal preconditioning. By maintaining a stable thermal environment,<sup>1</sup> we significantly reduce the risk of premature apoptosis, ensuring that the biological systems are in prime condition for their subsequent suborbital flights.

Proper ground studies on biological systems under diverse thermal conditions are crucial for designing and evaluating the reliability and performance of future space payloads. Many of these payloads must operate autonomously for extended periods, often without astronaut intervention. Prioritizing minimalism in design while optimizing hardware efficiency is essential. Our organization has experience in managing various biological systems that have matured through insights from successful suborbital missions with Blue Origin's New Shepard vehicle and NASA's airborne science initiatives. We have worked with several biological systems ranging from T-cells,<sup>2-3</sup> requiring a precise 37°C, to zebrafish embryos at 26-30°C,<sup>4</sup> and spirulina<sup>5</sup> thriving at 20-40°C, but our system could also provide thermal regulation to rodents at an average of 28.5°C (within a 22-30°C range) and flies (18-25°C).

In this paper, we will provide an assessment of a lab experiment with *Escherichia coli* using our thermal management system and a microbiological incubator as a reference for comparison. Then, we will compare the optical density (OD) and colony-forming unit (CFU) or bacteria cell count for both systems and provide recommendations for future experiments. OD and CFU serve to validate the effectiveness of our prototype. Optical density measures the turbidity or cloudiness of the culture, which correlates with the concentration of microbial cells present. By monitoring optical density over time, we can assess the growth kinetics of *E. coli* within our thermal management device. On the other hand, CFU involves plating a small post-incubation aliquot of a sample onto agar plates and counting the resulting colonies after incubation. This method allows for the enumeration of viable microorganisms present in the sample. Together, these techniques offer a significant estimate of the performance of our system by comparing it to the performance of a standard microbiological incubator.

Finally, we will provide an analysis of the different thermal stressors that can affect a CubeSat housing this specimen in orbit and how we can leverage these for both hot and cold case scenarios. Real-time monitoring of

microbial growth is crucial for assessing the risk of microbial contamination and ensuring that the air and water systems aboard spacecraft are free from harmful levels of bacteria and fungi. Understanding how bacteria grow in space can help develop strategies to control microbial contamination and improve the safety and efficacy of long-duration space missions. On the other hand, the estimation of viable cell counts is relevant to astronaut's health since water samples are regularly tested to ensure they do not contain harmful levels of microorganisms that could cause illness. Surfaces within the International Space Station (ISS) are swabbed and tested to monitor and control microbial contamination, which helps maintain a clean and safe environment for astronauts to live and work. Finally, understanding the growth dynamics of potentially pathogenic microorganisms can help in assessing the risk and preventing the spread of infections among the crew. By monitoring these parameters, astronauts can take proactive measures to prevent microbial growth that could compromise air and water quality, contribute to the degradation of spacecraft materials, or pose health risks to the crew. It is critical to monitor these variables in the closed and controlled environment of space missions where the immune response of astronauts can be altered by microgravity, and the potential for microbial cross-contamination is high due to the confined living and working quarters within the ISS.

The basic concept of our thermal management system (TMS) is the usage of a resistive heating thermal pad to warm a metal plate to which our bacteria samples are adhered. This approach relies on both contact and radiative heat transfer to warm the bacteria samples. Convective heating cannot be relied upon, since these air currents do not exist in a microgravity environment. On Earth, a minor amount of convective heat transfer occurs when the thermal pad is turned on, but this is kept to a minimum because the confined space within the TMS limits the amount of air needing to be warmed, and gravity-induced air currents are minimized. Our thermal management system (TMS) holds various temperature sensors and telemetry systems integrated within the transport containers to provide real-time monitoring through the liquid crystal displays (LCDs) of the payload conditions. This data can be used to make adjustments on the fly and ensure the payload remains within the required thermal parameters. This TMS significantly enhances the reliability and effectiveness of transporting biological payloads by providing real-time temperature monitoring, automated thermal adjustments, data logging and analysis, enhanced payload viability, and a proactive alert system. Biological samples can be easily accessible and integrated into the system within minutes. Thus, the integrity of the payloads is preserved from the point of origin to the launchpad, ultimately contributing to the success of space missions involving biological research.

## II. Methodology

### A. Thermal Management System

Specifications of the NanoLab (4U form factor) and Thermal Management System can be provided in Table 1:

**Table 1. The main parts of the thermal management system**

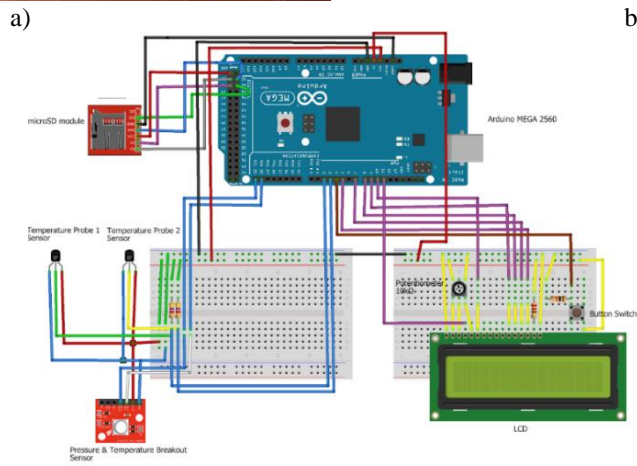
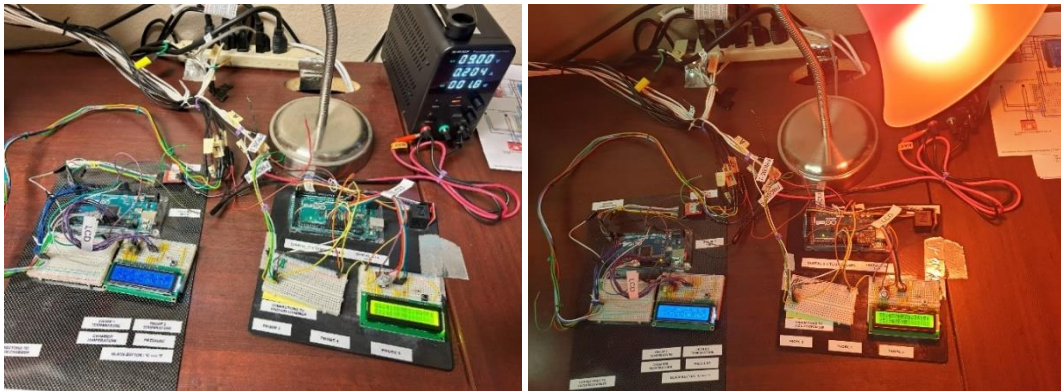
Thermal Management System	Specifications
NanoLab housing experiment (4U factor)	ABS premium 20cm × 20cm × 10cm
2 x Arduino	5.5 V
Thermal Sensors	3.3 V
2 x Liquid crystal display (LCD)	5.0 V
Average Amps with Heath Pad ON	0.220 A
Average Amps with Heath Pad OFF	0.213 A
Silicone heating pad	10 cm × 20 cm; 5V; 0.4W/cm <sup>2</sup>
Average power used	1.85 W
Beginning experiment temperature	22.2 °C
Ending experiment temperature	22.2 °C
Target temperature for bacteria	30.0 °C

The thermal management system (see Figure 1) shows a cyclic behavior when the thermal pad is ‘off’ (Figure 1a) and ‘on’ (Figure 1b, the lamp is on). The supporting electrical equipment (see Figure 1b), Figure 1c) could fit within another 2U (20cm × 20cm × 10cm ) or 4U. Figure 1c displays the electrical diagram for thermal probes 1 and 2, and the breakout sensor. (The 4U NanoLab (20cm × 20cm × 10cm) houses the biological vials as shown in Figure

1d. A lid (not shown in Figure 1d) covers the NanoLab to ensure heat remains within the NanoLab. Both NanoLab and lid are 3D printed with Acrylonitrile Butadiene Styrene (ABS) premium. Figure 1e shows an example of two bacteria samples at the start (more transparent) and end (more cloudy) of the experimental run. Figure 1f depicts the location of the five bacteria sample tubes on the thermal pad. Figure 1g displays the location a single bacteria sample tube on the thermal pad. The TMS is located in the Payload Applied Technology and Operations (PATO) Lab.

We conducted seven thermal biological tests in the PATO lab. Runs one to three used a single thermal sensor. For these first three runs, we used a single incubator as the main reference to compare the experimental samples of the thermal management system.

Runs four to seven used five sensors spread out above the heating pad which sat on top of an aluminum plate to ensure thermal temperature distribution as even as possible. By increasing the number of thermal sensors, we introduced greater redundancy into the system, which in turn enhanced the reliability of science operations. More sensors mean that we can more accurately monitor temperature fluctuations across different parts of the equipment, ensuring that all components operate within their optimal thermal ranges. This redundancy allows for detecting and compensating any sensor failures or anomalies, ensuring continuous and accurate data collection. Consequently, the increased precision in temperature control directly contributes to the stability and reliability of the experiments conducted, leading to more reliable scientific outcomes. Thus, the addition of more thermal sensors reduces the risk of data loss or experimental error due to temperature-related issues, bolstering the overall integrity of the science operations. For these three tests, we added the same number of samples inside an additional incubator reference (thermal oven). Then, all sample's thermal profiles, colony-forming units, and optical density are analyzed and interpreted. Thus, there were fifteen samples in total (five as reference in the incubator, five in the thermal oven, five in the NanoLab). Each bacteria sample was taped together with a thermal sensor, also taped to the heating pad as displayed in Figure 1d. Each bacteria sample is assigned a temperature probe, which is important for determining the local temperature of each bacteria sample and how it impacts the bacteria growth rate.



c)

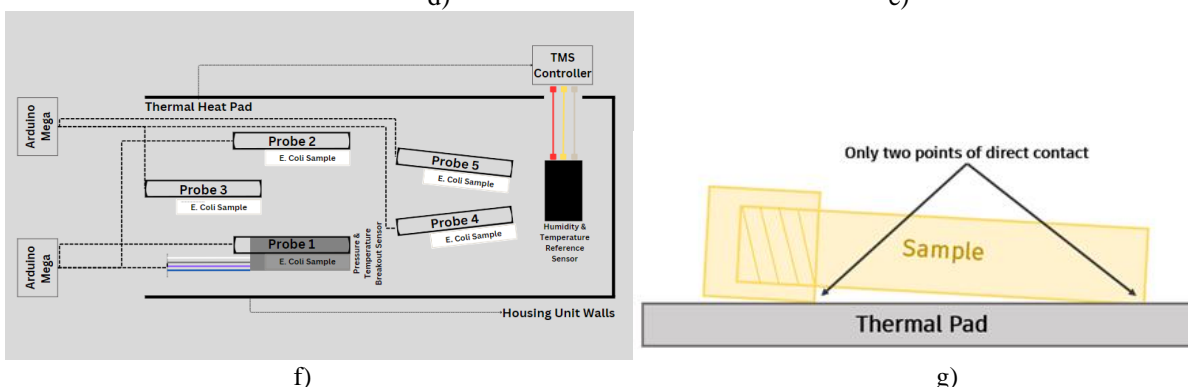
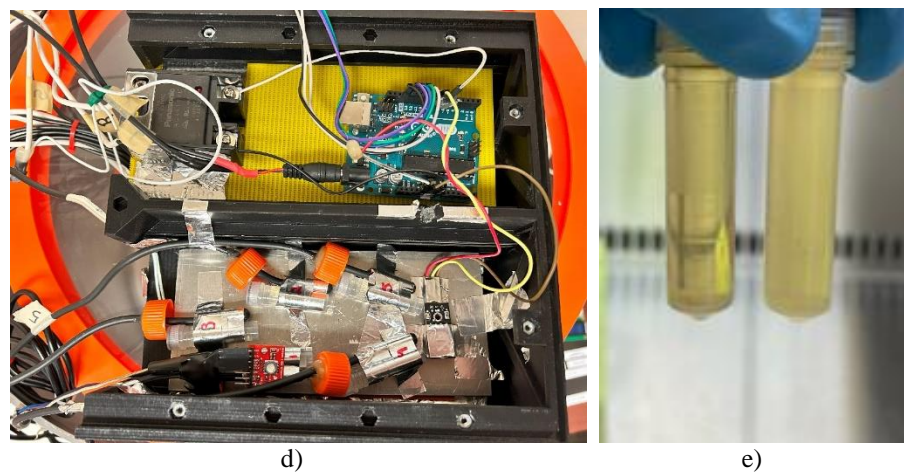


**Figure 1. Set up of the thermal management system. a) The thermal pad is OFF (no red light). b) The thermal pad is ON as indicated by the red light. c) Diagram depicting electrical configurations for the TMS. d) Location of tubes on the aluminum plate atop the thermal pad. e) Comparison of E. coli at the beginning (left) and end of incubation (right). f) Diagram showing placement of probes on the thermal pad. g) Diagram showing placement of a sample on the thermal pad.**

Note that Figure 1c displays configurations for probes 1, 2, and the breakout sensor. The configurations for probes 3, 4, and 5, are the same as depicted in Figure 1c with probe 5 in place of the breakout sensor.

It is important to note the location of the probes on the thermal pad because later on we will discuss any differences in growth that depend on location and temperature variability.

## **B. Bacterial growth: Optical Density and Colony-Forming Units**

The optical density (OD) at 630 nm is a measure of the total number of cells growing suspended in liquid culture, while plate count estimates the number of viable cells. In preparation for validation experiments, overnight cultures (OC) were prepared by inoculating 2 mL of nutrient broth (5% peptone, 3% beef extract, 1% sodium chloride) with a single colony from an *Escherichia coli* K12 reference plate and grown at 30°C and 200 rpm on an orbital shaker for 15 h, the standard protocol to provide cells with ample quantities of oxygen and nutrients and promote optimal growth prior initiating an experiment. On the day of the experiment, the OC was diluted 1:100 in nutrient broth and 2 mL aliquots were transferred into 2 mL screw-cap sterile tubes and transferred to the NanoLab, microbiological incubator, and oven and incubated for 12, 24, or 48 h. After the experiment, 100 µL aliquots were transferred into two wells of a 96-well plate to measure the optical density at 630 nm in wavelength using a microplate reader. The cell count was estimated by the serial dilution of the samples and plating 10 µL drops, in triplicate, on nutrient agar (nutrient broth solidified with 1.5% agar). The plates were incubated at 30° C for 15 h and the colonies were counted to calculate the colony-forming units per mL (CFU/mL). The samples from the reference incubator were processed in the Space Microbiology (SM) Lab. The NanoLab samples were processed in the SM lab, and brought to the PATO lab, and placed in the TMS during a five-minute walk.

### III. Results

#### A. Thermal Biological Tests, OD, and CFU

In this section, we provide some preliminary results from our dry test runs as displayed in Table 2:

**Table 2. Thermal results for dry test runs: Average temperature  $\pm$  SD ( $^{\circ}$ C)**

Test Run	Sensor 1	Sensor 2	Sensor 3	Sensor 4	Sensor 5
1	30.05 $\pm$ 0.68	NA	NA	NA	NA
2	30.44 $\pm$ 0.90	NA	NA	NA	NA
3	30.71 $\pm$ 0.49	NA	NA	NA	NA
4	32.33 $\pm$ 1.17	31.85 $\pm$ 1.16	31.16 $\pm$ 0.97	32.27 $\pm$ 1.02	28.84 $\pm$ 0.74
5	31.28 $\pm$ 1.03	31.52 $\pm$ 1.10	29.84 $\pm$ 0.63	31.04 $\pm$ 0.71	30.64 $\pm$ 0.76
6	28.00 $\pm$ 0.48	25.77 $\pm$ 0.36	29.76 $\pm$ 0.32	29.77 $\pm$ 0.32	29.99 $\pm$ 0.34
7	failed	failed	29.48 $\pm$ 0.35	30.54 $\pm$ 0.38	30.58 $\pm$ 0.39
8	30.49 $\pm$ 1.05	failed	29.83 $\pm$ 0.57	30.93 $\pm$ 0.62	30.82 $\pm$ 0.62
9	failed	failed	30.25 $\pm$ 0.49	30.80 $\pm$ 0.49	30.58 $\pm$ 0.49

The first three runs had a single sensor. These runs were preliminary runs to test our equipment. Runs 4-9 had five sensors. Figure 2 shows the thermal profile for a single probe sensor placed on the thermal pad targeting an average temperature of 30.05 $\pm$ 0.68 $^{\circ}$ C, and a probe 2 sensor placed under the lid of the NanoLab reaching a temperature near 26 $^{\circ}$ C. Thus, the mean temperature for each of the four samples corresponding to the CFU and OD profiles as seen in Figure 2b) and Figure 2c), respectively, is the temperature measured by probe sensor 2 for samples 2-4, and the temperature measured by probe sensor 1 is for sample 1.

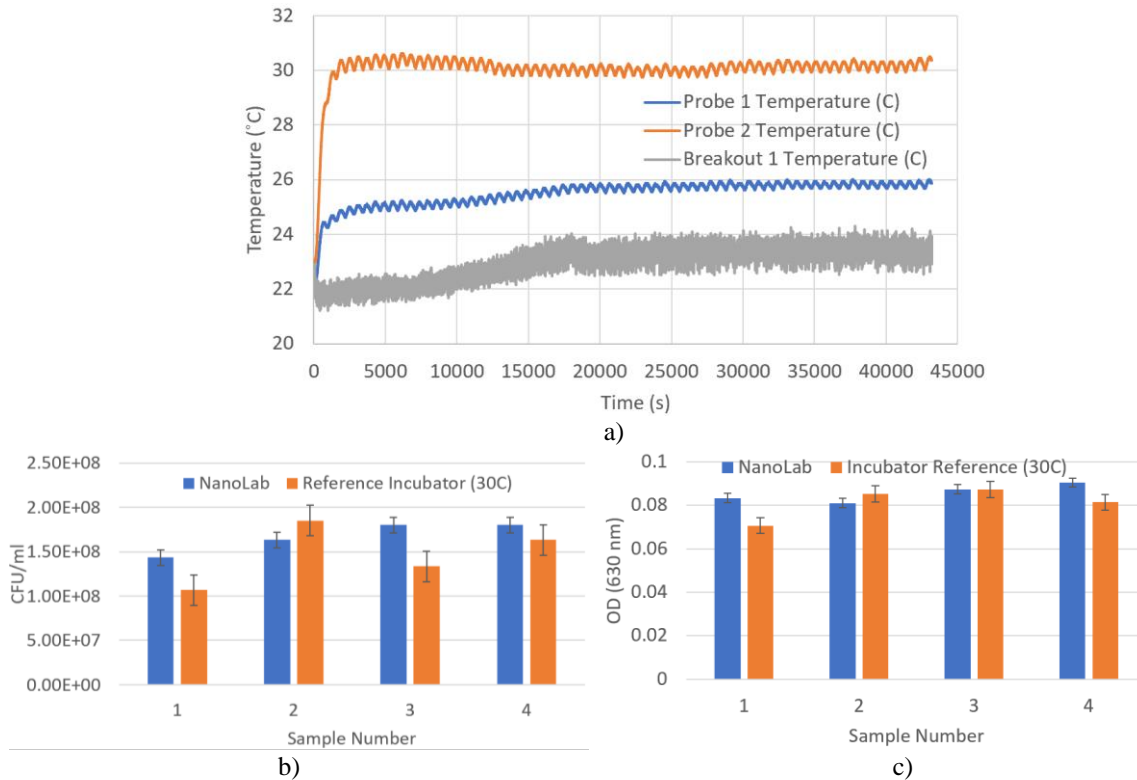


**Figure 2. First biological thermal test. a) Temperature profiles for sensors. b) CFU for NanoLab and incubator samples. c) Optical density for NanoLab and incubator samples.**

The lowest CFU and OD correspond to sample 1 (location of probe 1 sensor) while the CFU and OD for the other three samples (location of probe sensor 2) show higher consistency. The average OD for samples 2-4 were  $0.086\pm 0.006$  and  $0.085\pm 0.002$  for the NanoLab and reference incubator, respectively.

Similar observations can be extracted from the 12-hour test displayed in Figure 3, where the number of samples was increased to five in the NanoLab while keeping a single sample under the lid of the NanoLab. The average temperature profile for samples 2-6 as measured by a single sensor was  $30.44\pm 0.90^\circ\text{C}$ . The average OD for samples 2-6 were  $0.081\pm 0.002$  and  $0.076\pm 0.002$  for the NanoLab and reference incubator, respectively.

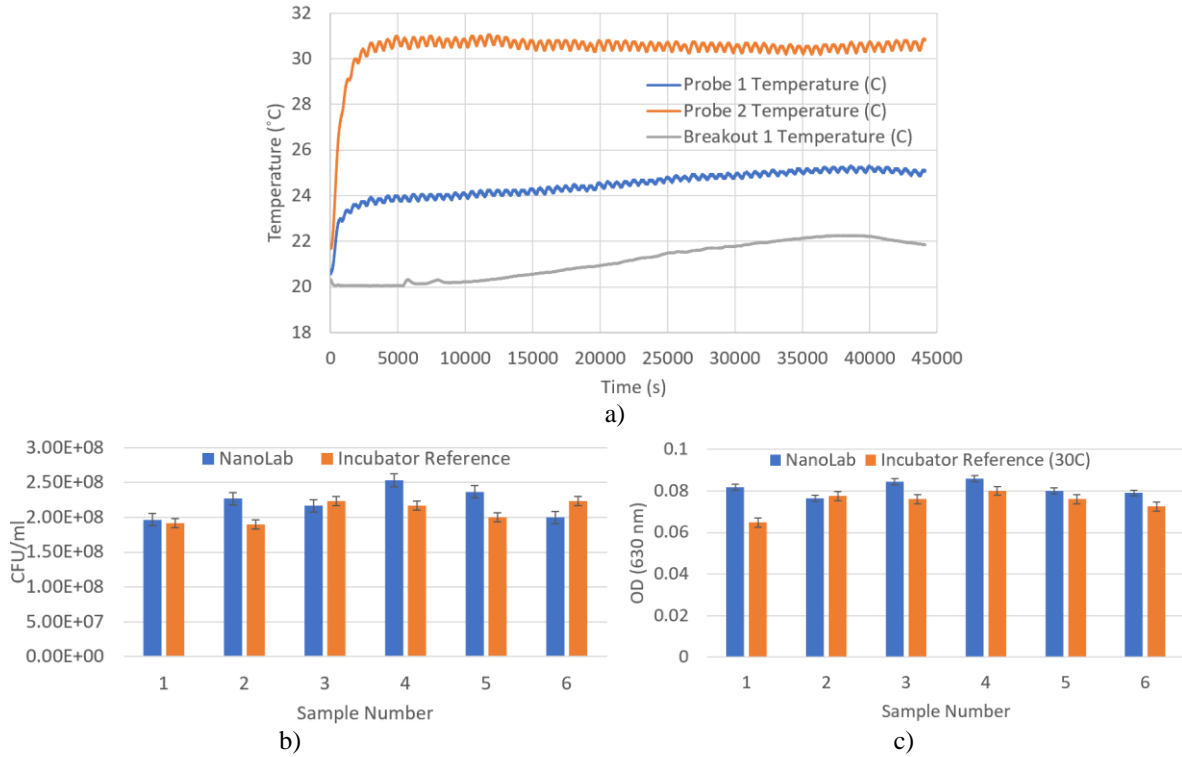


**Figure 3. Second biological thermal test. a) Temperature profiles for sensors. b) CFU for NanoLab and incubator samples. c) Optical density for NanoLab and incubator samples.**

The team conducted another 12-hour test (see Figure 4) with another six samples, five of which were atop the thermal pad, and a single one was under the lid of the NanoLab. The average temperature profile for samples 4-8 as measured by a single sensor was  $30.71\pm 0.49^\circ\text{C}$ . The average OD for samples 4-8 were  $0.1011\pm 0.0004$  and  $0.0966\pm 0.0014$  for the NanoLab and reference incubator, respectively.



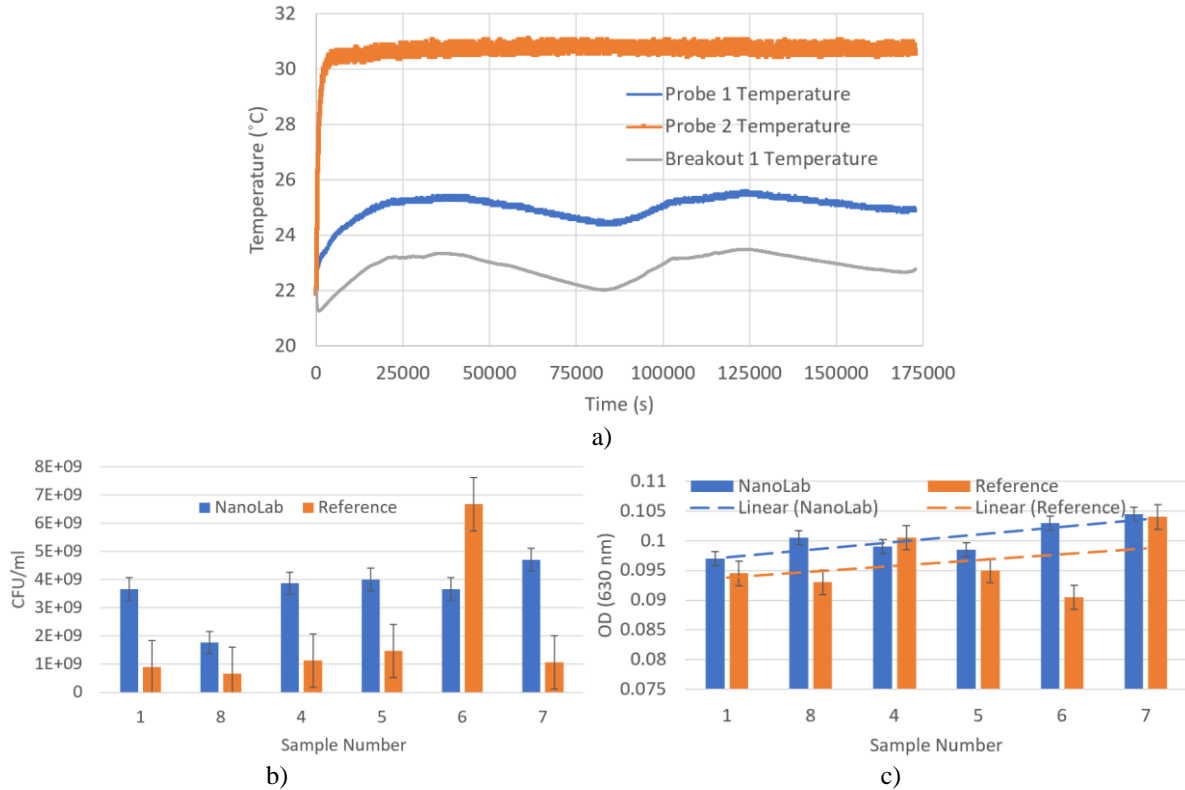


**Figure 4. Third biological thermal test. a) Temperature profiles for sensors. b) CFU for NanoLab and incubator samples. c) Optical density for NanoLab and incubator samples.**

In subsequent tests, we had several probes, and we will be able to compare each thermal profile for each CFU and OD profile. For this third test run, we obtained a CFU/ml average of  $1.67E+08$  and  $1.47E+08$  for both the NanoLab and reference incubator, respectively.

Two 24-hour tests (see Figure 5) were conducted with another five samples per test, all samples were atop the thermal pad-aluminum plate subsystem. For the first run, the average temperature profile for all six samples as measured by five probe sensors were  $31.28 \pm 1.03^\circ\text{C}$ ,  $31.52 \pm 1.10^\circ\text{C}$ ,  $29.84 \pm 0.64^\circ\text{C}$ ,  $31.04 \pm 0.71^\circ\text{C}$  and  $30.64 \pm 0.76^\circ\text{C}$ , for sensors 1 to 5, respectively. In the first test run, the average OD for samples 1-5 were  $0.2579 \pm 0.0123$  and  $0.1688 \pm 0.0017$  for the NanoLab and reference incubator, respectively. For the second run, the average temperature profile for all six samples as measured by five probe sensors were  $32.33 \pm 1.17^\circ\text{C}$ ,  $31.85 \pm 1.16^\circ\text{C}$ ,  $31.16 \pm 0.97^\circ\text{C}$ ,  $32.27 \pm 1.02^\circ\text{C}$  and  $28.84 \pm 0.74^\circ\text{C}$ , for sensors 1 to 5, respectively. In the second test run, the average OD for samples 1-5 were  $0.2643 \pm 0.0097$  and  $0.1670 \pm 0.0018$  for the NanoLab and reference incubator, respectively. Note that although two of the probe sensors failed to provide thermal data for about 10 hours, the profile was consistent from the commencement until the end of the run. Thus, we assumed that the temperature profile was the same during the lost data. It is important to note that the thermal profiles obtained in the NanoLab were about  $1.5\text{-}2^\circ\text{C}$  higher than the targeted temperature of  $30^\circ\text{C}$  (reference incubator), hence the OD is expected to be higher yielding greater viability on the NanoLab samples.

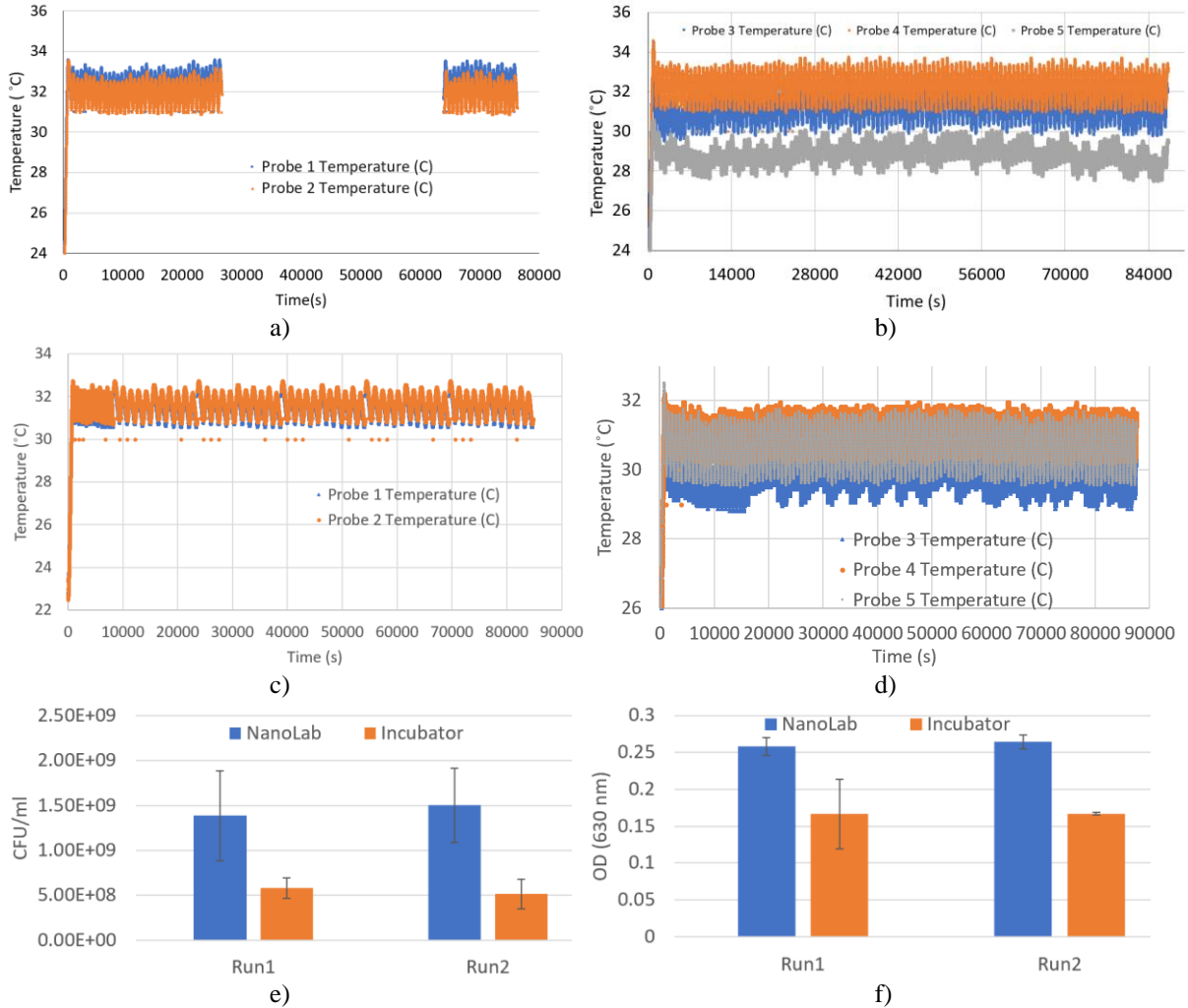


**Figure 5. Fourth and fifth biological thermal tests. a) Temperature profiles for sensors 1 and 2 of run 1. b) Temperature profiles for sensors 3, 4, and 5 of run 1. c) Temperature profiles for sensors 1 and 2 of run 2. d) Temperature profiles for sensors 3, 4 and 5 of run 2. e) Comparison between runs 1 and 2 of CFU for NanoLab and incubator samples. f) Comparison between runs 1 and 2 optical density for NanoLab and incubator samples.**

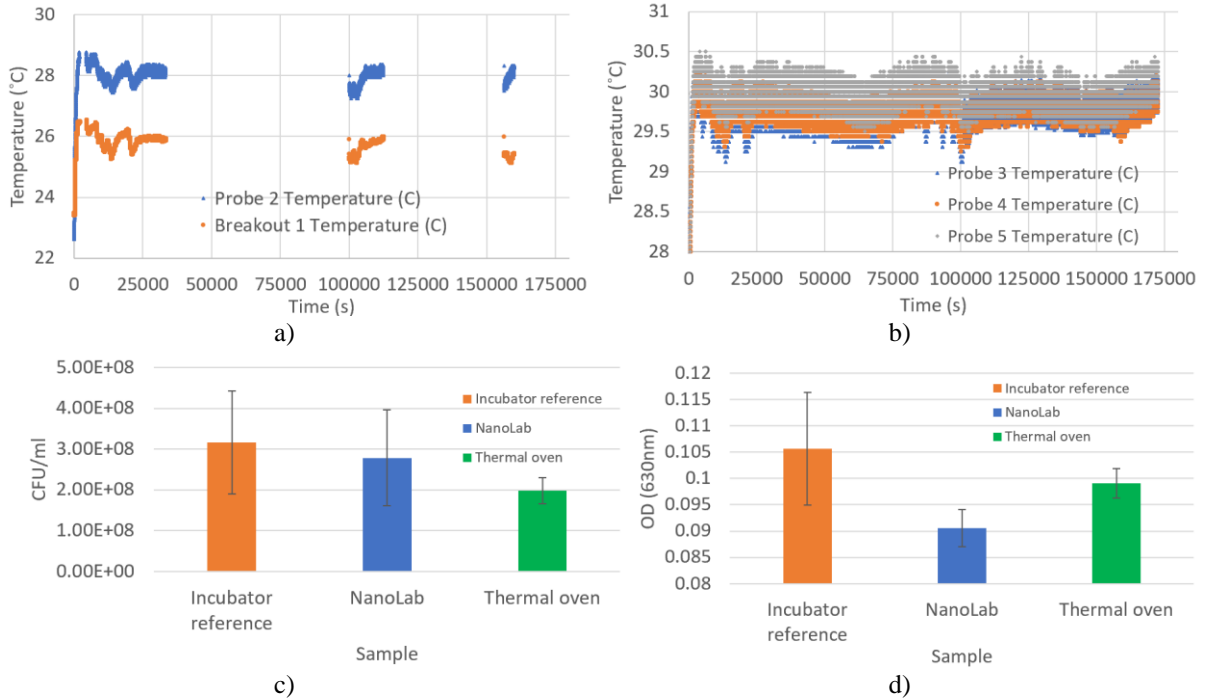


**Figure 6. Sixth biological thermal test. a) Temperature profiles for sensors 1 and 2. b) Temperature profiles for sensors 3, 4, and 5. c) Comparison of CFU across samples in the NanoLab, incubator, and thermal oven. d) Comparison of optical density across samples in the NanoLab, incubator, and thermal oven.**

Probes 1 and 2 failed but provided intermittent data enough to be used to assess the consistency of thermal profiles.

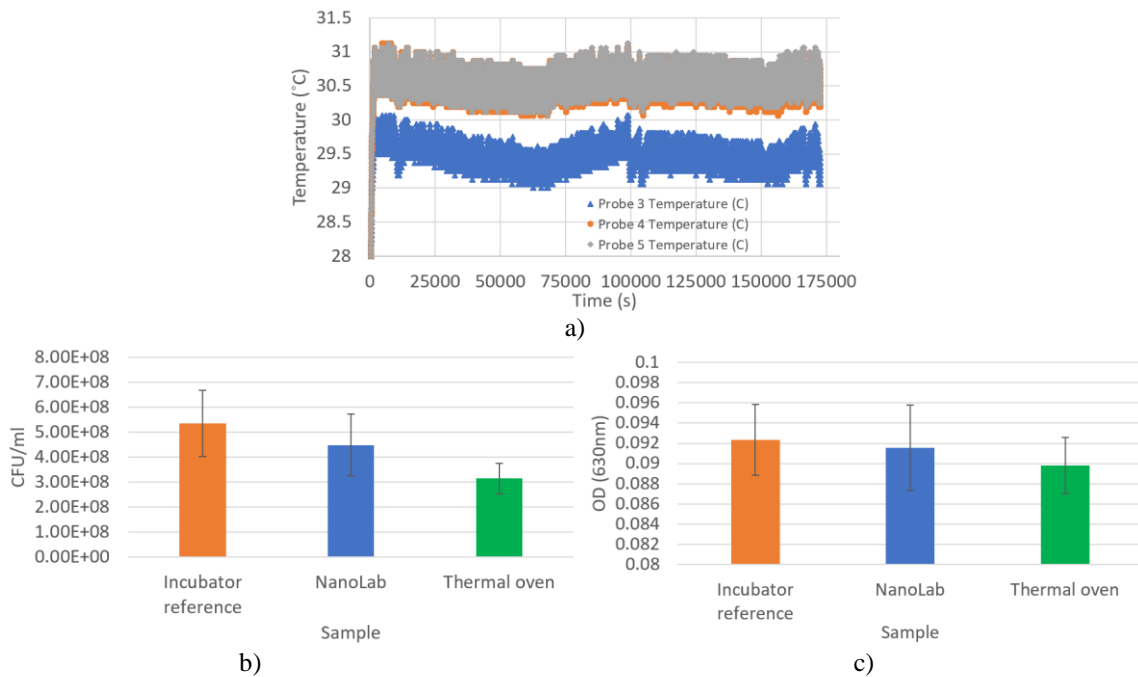


**Figure 7. Seventh biological thermal test. a) Temperature profiles for sensors 3, 4, and 5. b) Comparison of CFU across samples in the NanoLab, incubator, and thermal oven. c) Comparison of optical density across samples in the NanoLab, incubator, and thermal oven.**

In Figure 6 and Figure 7, we display two 48-hour tests. In each test, we had five samples in the reference incubator and five samples in the NanoLab and we added another five into another thermal oven configuration in the same laboratory where the NanoLab is to add more consistency with all samples across. In the first 48-hour test, the averages of OD for the reference incubator, NanoLab, and thermal oven configurations were  $0.106\pm 0.011$ ,  $0.091\pm 0.004$  and  $0.099\pm 0.003$ , respectively. In the second 48-hour test, the averages of OD were  $0.0923\pm 0.0035$ ,  $0.0915\pm 0.0042$ , and  $0.0898\pm 0.0028$ , respectively. OD results were very consistent across all conditions.

The average temperature for all five probe sensors were  $28.00\pm 0.48^\circ\text{C}$ ,  $25.77\pm 0.36^\circ\text{C}$ ,  $29.76\pm 0.32^\circ\text{C}$ ,  $29.77\pm 0.32^\circ\text{C}$  and  $29.99\pm 0.34^\circ\text{C}$ , respectively during the sixth test. Note that the temperatures for the first two probes are lower than expected because they were not properly taped to the thermal plate, resulting in them hovering about half an inch above the plate. This positioning means the probes do not heat as much due to reduced heat transfer. In the seventh test, the average temperatures for probes  $29.48\pm 0.35^\circ\text{C}$ ,  $30.54\pm 0.38^\circ\text{C}$  and  $30.58\pm 0.39^\circ\text{C}$ , for sensors 3 to 5, respectively, since probes 1 and 2 failed to provide any data.

The five samples inside the thermal oven were placed at the bottom of the oven, so we cannot rule out that they might have been shown a slightly higher temperature because of the instruments underlying the thermal oven which might have added a slight increase in temperature, however, further analysis needs to be assessed (eg. placing another inside thermal probe inside the thermal oven). The mean of all five samples is provided.

Figure 8a)-b) displays the averaged CFU and OD for all tests conducted at each time configuration (12h, 24h, and 48h). Our results suggest that the highest OD of bacteria was obtained around 24 hours, perhaps due to the slightly higher temperatures at which the samples were exposed in the NanoLab, and for the 12 hours and 48-hour period, the OD was very close to the one in the reference incubator. Temperature determines the optimal enzymatic activity and membrane fluidity in bacteria that lead to optimal growth<sup>6,7</sup> hence the importance of thermal control.

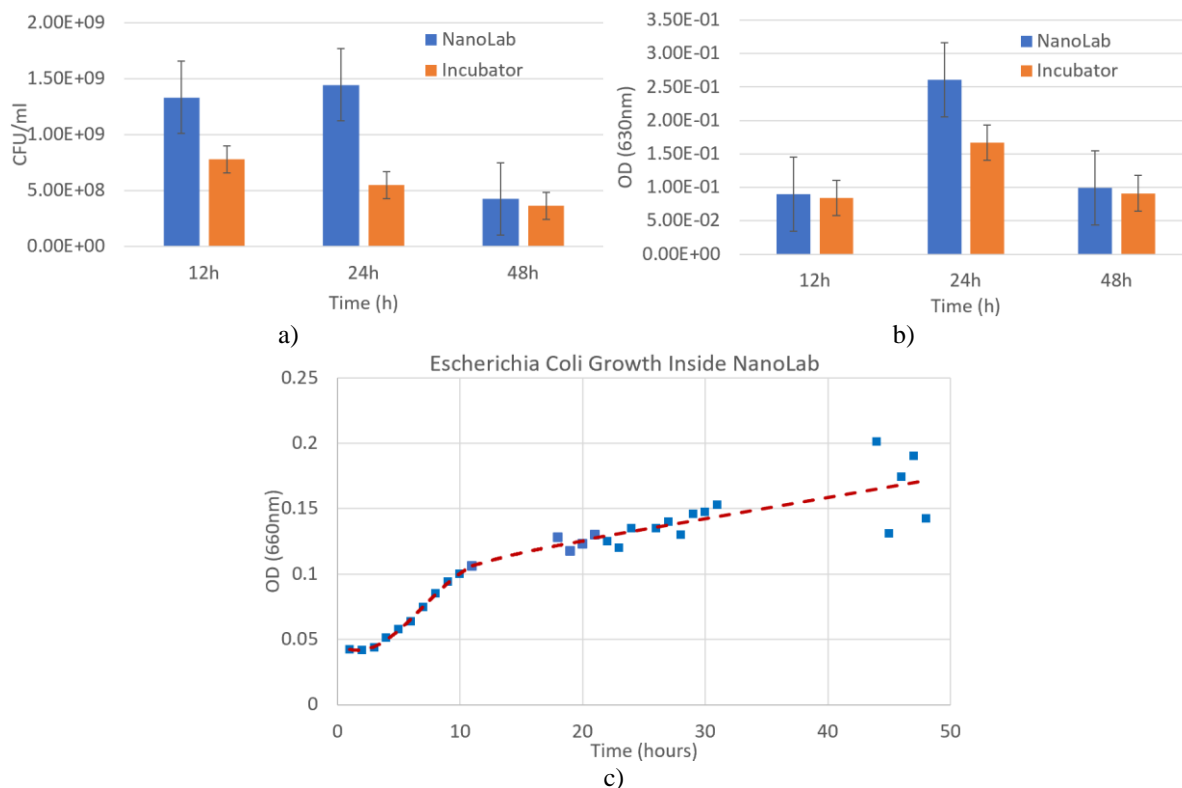


**Figure 8. a) Averaged CFU for all 12-hour, 24-hour, and 48 tests. b) Averaged OD for all 12-hour, 24-hour, and 48 tests. c) Growth curve of Escherichia Coli for samples inside of NanoLab.**

Two additional 24-hour tests (tests 8 and 9, respectively) were conducted. In contrast to previous tests, where the bacteria samples were positioned solely in one corner at the base of the thermal oven, tests 8 and 9 involved placing the bacteria samples at the center of the thermal oven like the bacteria samples located in the reference incubator. This

adjustment was made to ensure a more uniform distribution of heat throughout the sample. The first test yielded consistent thermal stability with averages (sensors 3, 4, and 5) of  $29.83\pm 0.57^{\circ}\text{C}$ ,  $30.93\pm 0.62^{\circ}\text{C}$ , and  $30.82\pm 0.62^{\circ}\text{C}$  for test 8, and  $30.25\pm 0.49^{\circ}\text{C}$ ,  $30.80\pm 0.49^{\circ}\text{C}$ ,  $30.58\pm 0.49^{\circ}\text{C}$ , for test 9, respectively. In the eighth and ninth test runs, the average OD for both sets of samples were  $0.1910\pm 0.0178$ ,  $0.1581\pm 0.0142$ , and  $0.1670\pm 0.0103$  for the NanoLab, reference incubator, and thermal oven, respectively. Similarly, the CFU/ml are  $3.58\times 10^9\pm 2.24\times 10^9$ ,  $5.19\times 10^9\pm 2.78\times 10^9$ , and  $3.00\times 10^9\pm 1.48\times 10^9$ , respectively. The next step would be to analyze all the pooled experiments as shown in Table 3 and Table 4.

**Table 3. Optical Density for all runs (pooled experiments)**

Time of Runs	t-test	NanoLab	Reference Incubator	Oven
12h	Mean	0.092	0.086	
	Standard Error	0.002	0.002	
	t-test	0.000		
24h	Mean	0.235	0.161	0.167
	Standard Error	0.007	0.004	0.004
	t-test	0.000		
48h	Mean	0.091	0.099	0.094
	Standard Error	0.001	0.002	0.001
	t-test	0.001		

**Table 4. Cell Count (CFU/ml) for all runs (pooled experiments)**

Time of Runs	t-test	NanoLab	Reference Incubator	Oven
12h	Mean	1.40E+09	8.16E+08	
	Standard Error	4.16E+08	3.69E+08	
	t-test	0.142		
24h	Mean	2.17E+09	2.87E+09	3.00E+09
	Standard Error	3.94E+08	1.16E+09	5.64E+08
	t-test	0.022		
48h	Mean	3.63E+08	4.26E+08	2.56E+08
	Standard Error	4.59E+07	5.31E+07	2.44E+07
	t-test	0.386		

The growth curve of *E. coli* in Figure 8c) can be dissected into distinct phases (lag, exponential, stationary, and death), each reflecting a different physiological state of the bacterial population. The lag phase represents a period of adaptation where bacteria adjust to their new environment, synthesizing necessary enzymes and molecules for growth. Following this, the exponential phase is characterized by rapid cell division, with bacteria doubling in number at a constant rate, reflecting their optimal growth conditions. As resources become limited and waste accumulates, the growth rate decreases, leading to the stationary phase, where cell division ceases, and the population stabilizes as the rate of cell growth equals the rate of cell death. Eventually, in the death phase, the depletion of nutrients and buildup of toxic byproducts cause the number of viable cells to decline, ultimately leading to cell death.

The lag phase (time frame: 0 to approximately 5 hours). The bacteria are adjusting to the surrounding environment. There is no significant increase in cell number; the cells are gearing up for growth by synthesizing new enzymes and nutrients required for cell division. The optical density (OD) remains relatively constant because the bacteria are not yet multiplying noticeably. The *E. coli* are acclimatizing to the conditions inside the NanoLab, such as temperature, pH, and nutrient availability. The curve's flatness indicates that the cells are metabolically active but not yet dividing rapidly.

The Log Phase (Exponential Phase) has a timeframe of approximately 5-20 hours. This phase shows a rapid increase in bacterial population density, reflected in the curve's sharp upward slope. During the log phase, the cells divide at a constant and maximum rate. The growth rate depends on the conditions provided and is characterized by a continuous doubling time. The conditions in the NanoLab support robust bacterial growth, and *E. coli* are replicating rapidly. The steepness of the slope indicates healthy, exponential growth, with cell numbers doubling at regular

intervals. This is the phase where *E. coli* is most susceptible to antibiotics and is typically the target phase for studying bacterial genetics and metabolism.

The stationary phase typically spans from approximately 20 to 48 hours. During this period, the growth rate of the bacterial population decelerates, and the growth curve flattens, indicating a balance between cell replication and cell death. Several stress factors contribute to this equilibrium, including nutrient depletion, accumulation of toxic metabolites, and spatial constraints. It is plausible that in the NanoLab environment, the *E. coli* culture has depleted available nutrients or accumulated waste products to inhibitory levels, halting further growth. Consequently, the bacteria may undergo metabolic adjustments, prioritizing survival mechanisms over proliferation. Despite the cessation of cell proliferation, significant biological activities persist during this phase, such as alterations in gene expression and activation of stress response pathways. Another interesting observation can be extracted from Figure 8c). During the first 10 hours (initial lag and early log phase), the data points follow the growth curve (red dashed), the next set of data points from 18 hours to 31 hours (mid to late log phase) shows a slight variability, and the last set of data points approximately above 40 hours (stationary phase) shows the highest variability.

The NanoLab's thermal control exhibited consistent stability, maintaining optimal temperature conditions for *E. coli* over 48 hours, as evidenced by the summarized growth of our biological model. Table 3 indicates no significant disparity in optical density between the 12 and 48-hour experiments. However, during the 24-hour trials, there was a notable uptick in absorbance, implying an unexpected temperature elevation that likely accelerated the growth rate and cell accumulation compared to other time intervals. Nevertheless, this disparity was not mirrored in the final count of viable cells after each incubation period, as depicted in Table 4. Several factors could contribute to this discrepancy, including temperature fluctuations leading to cell aggregation or variations in cell morphology within the 24-hour cultures, thereby altering light scattering properties (resulting in increased OD) without a corresponding rise in cell count (no change in CFU/mL).

## B. Power Budget for Thermal Management System

Understanding the power consumption required to maintain a habitable environment for both the crew and microorganisms, such as bacteria, is essential. It is equally important to ensure the survival of the biological system under controlled environmental conditions. For example, the Veggie plant growth unit aboard the ISS draws about 115 W peak power. The wattage for this system is about 2760 W-hr if continuously used for 24 hours.

Table 5 displays some relevant tests, the length of each test, the number of times the thermal pad was on, the total time it was on, the percentage of hours it was on, the number of hours it was on, and the wattage. For example, the total wattage for test five was 7.0 W-hr. For example, test seven duration was 48 hours. During this test, the thermal pad was turned ON 3286 times. Since the duration of the thermal pad each time is turned ON is about 5.1 seconds, then,  $(3286) \cdot (5.1) = 18730$  seconds (4.65 hours). The wattage (W-hr) is obtained by multiplying the number of hours times 1.85 W, which is the average power of the thermal pad 1.85W.

**Table 5. Thermal Pad performance for some thermal biological tests**

Test	Duration of test (h)	Number of times thermal pad ON	# hours ON	Wattage (W-hr)
5	24	2676	3.77	7.0
6	48	3263	4.588	8.5
7	48	3286	4.635	8.6
8	24	1517	2.133	3.95
9	24	2015	6.752	12.49

In the future, the team intends to enhance the precision of the thermal control system through further optimization. Specifically, we aim to subject the entire system to controlled temperature fluctuation cycles and rigorously assess its performance improvements based on these tests.

## IV. Conclusion

The development of the ongoing thermal management system has proven effective in maintaining the temperature of a specific biological system within a NanoLab environment, achieving a commendable level of precision with less than 1°C (sometimes less than 0.5°C) average deviation in most experimental conditions. This precision is facilitated

by the incorporation of redundant sensors, ensuring reliability and consistency in temperature regulation. The scalability of our system is a notable advantage, as it offers potential solutions for mitigating thermal fluctuations that payloads encounter during transit between various institutions and the payload processing facilities at the launch site. Furthermore, our design demonstrates compatibility with small satellite formats, specifically fitting within the dimensional constraints of 4U to 6U CubeSats.

Looking forward, we propose to extend our research by conducting thermal simulations for a 6U CubeSat in orbit over multiple days. This will allow us to evaluate the effects of various orbital configurations, related thermal variations, and the efficacy of different CubeSat materials in managing these changes.

We aim to refine thermal inputs within the CubeSat, thereby deepening our understanding of how thermal sources impact enclosed biological systems. This future endeavor is geared towards enhancing our thermal management strategies to ensure they are more adaptable and more effective in addressing the demanding conditions of space.

### Acknowledgments

The researchers would like to thank the Applied Aviation Sciences Department's Payload Applied Technology and Operations Lab and the College of Arts and Sciences' Space Microbiology Lab.

### References

<sup>1</sup>Pedro J. Llanos, Vijay Vishal Duraisamy, Nikita L. Amberkar, Justin Nafziger, Cynthia Stockton, "Characterization of a Thermal Management System to Support Biological Payloads," AIAA 2022-1566, *AIAA SciTech Forum*, San Diego, CA, January, 2022. DOI:10.2514/6.2022-1566

<sup>2</sup>Pedro J. Llanos, Kristina Andrijauskaite, Vijay Duraisamy, Sathya Gangadharan, Jay Morris, Michael J. Wargovich, "Microgravity effect on murine T cells exposed to suborbital flight aboard Blue Origin's New Shepard vehicle," *Preprint server for biology* (bioRxiv) doi: <https://doi.org/10.1101/2021.05.13.443970>

<sup>3</sup>Pedro J. Llanos, Kristina Andrijauskaite, Vijay Duraisamy, Francisco Pastrana, Mark Rubinstein, Erik Seedhouse, Sathya Gangadharan, Leonid Bunegin, Mariel Rico, "Challenges of ERAU's First Suborbital Flight Aboard Blue Origin's New Shepard M7 for the Cell Research Experiment In Microgravity (CRExIM)," *Gravitational and Space Research*, GSR 58, 2019, 1-12. DOI:10.2478/gsr-2019-0001

<sup>4</sup>Pedro Llanos, Kristina Andrijauskaite, Mark Rubinstein, Sherine Chan, "Investigation of Zebrafish Larvae Behavior as Precursor for Suborbital Flights: Feasibility Study," *Gravitational and Space Research*, Volume 6 (1): 37-57, 2018. DOI: <https://doi.org/10.2478/gsr-2018-0004>

<sup>5</sup>Pedro Llanos, Morgan Shilling, Kody Kidder, Kristina Andrijauskaite, Dylan Orth, Vijay Duraisamy, "Assessment of Scientific Payload Carrying Spirulina Onboard Blue Origin's New Shepard Vehicle," *Global Journal of Research in Engineering (B)*, Vol 22, Issue 1, 1-15, 2022. DOI: 10.17406/GJRE

<sup>6</sup>Ratkowsky DA, Olley J, McMeekin TA, Ball A. Relationship between temperature and growth rate of bacterial cultures. *J Bacteriol*. 1982 Jan;149(1):1-5. doi: 10.1128/jb.149.1.1-5.1982. PMID: 7054139; PMCID: PMC216584.

<sup>7</sup>Zwietering MH, de Wit JC, Cuppers HG, van 't Riet K. Modeling of bacterial growth with shifts in temperature. *Appl Environ Microbiol*. 1994 Jan;60(1):204-13. doi: 10.1128/aem.60.1.204-213.1994. PMID: 16349151; PMCID: PMC201290.